Journal of Alloys and Compounds 509 (2011) 5263–5268

Contents lists available at ScienceDirect

Journal of Alloys and Compounds

journal homepage: www.elsevier.com/locate/jallcom

Rapid solidification and phase stability evaluation of Ti–Si–B alloys

K.C.G. Candioto[a,b,*], C.A. Nunes[a], G.C. Coelho[a,c], P.A. Suzuki[a], S.B. Gabriel[c]

[a] USP – Universidade de São Paulo (EEL), Lorena, SP, Brazil[1]
[b] AEDB – Associação Educacional Dom Bosco, Resende, RJ, Brazil[2]
[c] NUPE, UniFoa – Centro Universitário de Volta Redonda, Volta Redonda, RJ, Brazil

ARTICLE INFO

Article history:
Received 28 September 2010
Received in revised form 6 February 2011
Accepted 7 February 2011
Available online 17 February 2011

Keywords:
Rapid solidification
Ti–Si–B alloy
Amorphous alloy
Nanocrystal
HRTEM
DSC

ABSTRACT

Ti-rich Ti–Si–B alloys can be considered for structural applications at high temperatures (max. 700 °C), however, phase equilibria data is reported only for T = 1250 °C. Thus, in this work the phase stability of this system has been evaluated at 700 °C. In order to attain equilibrium conditions in shorter time, rapid solidified samples have been prepared and carefully characterized. The microstructural characterization of the produced materials were based on X-ray diffraction (XRD), scanning electron microscopy (SEM-BSE), high resolution transmission electron microscopy (HRTEM), High Temperature X-ray diffraction with Synchrotron radiation (XRDSR) and Differential Scanning Calorimetry (DSC). Amorphous and amorphous with embedded nanocrystals have been observed after rapid solidification from specific alloy compositions. The values of the crystallization temperature (Tx) of the alloys were in the 509–647 °C temperature range. After Differential Scanning Calorimetry and High Temperature X-ray Diffraction with Synchrotron radiation, the alloys showed crystalline and basically formed by two or three of the following phases: αTi, Ti_6Si_2B; Ti_5Si_3; Ti_3Si and TiB. It has been shown the stability of the Ti_3Si and Ti_6Si_2B phases at 700 °C and the proposition of an isothermal section at this temperature.

1. Introduction

Considering the potential application of Ti and its alloys at high temperatures [1–3], which in general is up to 700 °C, it has been decided to investigate the Ti–Si–B system [4,5] in terms of phase stability. Previous studies [4–6] have shown the phase equilibria of this system at 1250 °C in the Ti-rich region, where a ternary intermetallic phase Ti_6Si_2B-phase is in equilibrium with Ti_{ss} (ss-solid solution), Ti_5Si_3 and TiB [4,6]. However, there is no information concerning the phase equilibria at lower temperatures, where these alloys could be possibly applied. According to our previous investigations, it is considerably difficult to produce stable microstructures at lower temperatures and reasonable times from arc-melted samples, due to an initially coarse microstructure and sluggish diffusion. Thus, in this study, it has been decided to prepare the samples via a rapid solidification process (splat-cooling).

Rapid solidification refers to rapidly cooling liquid metals with rates above 106 K s^{-1} and may result in one or more of the following: refinement of grain size (grain <1 μm); extension of solubility limits; formation of metastable phases; retention of high temperature phases and/or formation of amorphous/nanocrystalline materials. The use of rapidly solidification techniques allows the production of alloys with higher chemical homogeneity and very fine microstructure and is one of the techniques for production of amorphous material [7]. Studies in the literature show the formation of amorphous/nanocrystalline Ti alloys [7–13] through rapid solidification, however, there is no data available with regards to the Ti–Si–B system.

Thus, the aim of this study was to produce and characterize rapidly solidified Ti-rich Ti–Si–B alloys and to determine the phase relations of this system on the Ti-rich region at 700 °C from heat-treatment of the rapidly solidified samples.

2. Experimental

Fig. 1 shows the experimental procedure related to the production and characterization of the Ti–Si–B alloys used in this work.

2.1. Ingots production

The ingots (~5 g) were prepared from high purity materials, Ti (min. 99.3 wt.%), B (min. 99.5 wt.%) and Si (99.9999 wt.%) by arc melting in a water-cooled copper crucible under argon atmosphere (min. 99.995%). They were then broken and a mass of ~100 mg weighed for the production of spheres, also by arc melting, for the rapid solidification experiments.

2.2. Rapid solidification

Rapidly solidified (RS) disks were produced from the arc-melted spheres using a splat cooling equipment from Edmund Bühler under argon atmosphere (min. 99.995%).

* Corresponding author at: Tel.: +55 24 33601726.
E-mail address: katccg@hotmail.com (K.C.G. Candioto).
[1] Tel.: +55 12 3159 9900.
[2] Tel.: +55 24 3383 9000.

0925-8388/$ – see front matter © 2011 Elsevier B.V. All rights reserved.
doi:10.1016/j.jallcom.2011.02.042

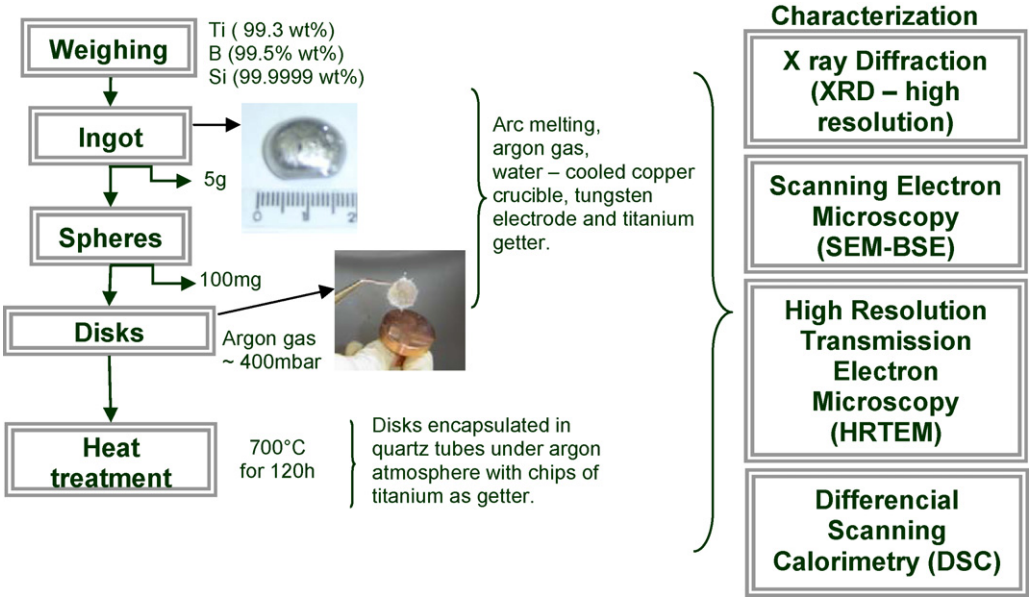

Fig. 1. Experimental procedure related to the production and characterization of the Ti–Si–B alloys.

2.3. Heat treatments

Some RS disks were encapsulated in quartz tubes with pieces of pure Ti (acting as $O_2/N_2/H_2O$ getter) under argon atmosphere (min. 99.995%). The heat treatments (HT) were carried out at 700 ° C for 120 h followed by air-cooling to room temperature.

2.4. Characterization

The microstructures of the ingots, spheres and disks were analyzed via scanning electron microscopy/back-scattered electrons mode (SEM/BSE) using an acceleration voltage of 20 kV in a LEO 1450VP SEM model. For those disks that could not have their microstructures solved via SEM, high-resolution transmission electron microscopy (HRTEM) was applied. The samples for HRTEM were prepared by electrolytic polishing (twin jet eletropolishing). The HRTEM evaluation was performed using an acceleration voltage of 300 kV in a JEOL JEM 3010 URP HRTEM model. DSC measurements from the RS disks were carried out in a SETARAM Setsys 1600 equipment under argon flow (min. 99.995%) with heating rate of 10 °C/min from room temperature to 750 °C and cooling rate of 20 °C/min. Alumina crucibles were used to contain the RS disks and empty alumina crucibles as references.

Conventional X-ray diffraction (XRD) was used to characterize the materials produced after each processing step. The XRD experiments were performed in a Shimadzu XRD6000 model at room temperature under Cu-Kα radiation and graphite monochromator.

Experiments of High Temperature X-ray diffraction with Synchrotron radiation (XRDSR) were performed from the RS disks at Brazilian Synchrotron Light Laboratory (LNLS) using 8 keV energy, Synchrotron radiation (λ = 1.5497 Å), resistive furnace and an image plate to capture the data. The experiments were performed under argon flow (min. 99.995%) from room temperature to 690 °C with heating rate of 10 °C/min and time exposure of 10 min at each isotherm to observe the crystallization of the amorphous phase.

3. Results and discussion

The alloys produced in this work were in the $Ti_{(100-x-y)}Si_xB_y$ ($5 \le x \le 28$ and $0 \le y \le 20$) composition range. Fig. 2 shows the 1250 °C isothermal section (superimposed) and the liquidus projection given by Ramos et al. [4] for the Ti–Si–B system.

3.1. Arc melted spheres

The microstructures of the spheres were all crystalline and formed by 2, 3 or 4 of the following phases: αTi, Ti_6Si_2B; Ti_5Si_3; Ti_3Si; TiB and TiB_2 (Table 1). In general, the phases present in a given alloy are in agreement with the expected from the liquidus projection proposed by Ramos et al. [4] for the Ti–Si–B system. The

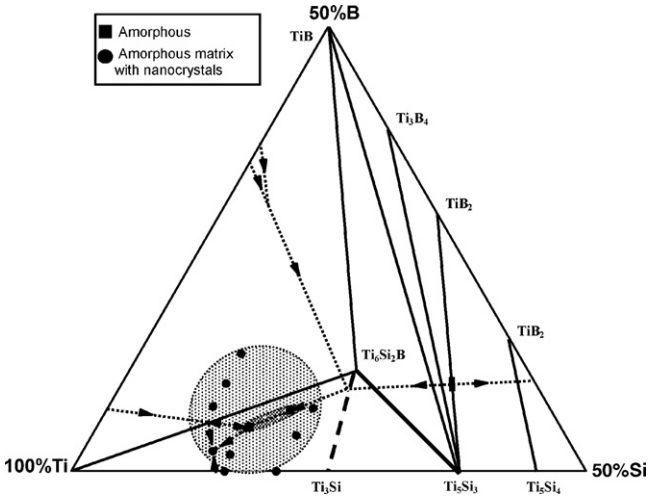

Fig. 2. 1250 °C isothermal section and the liquidus projection (dot line) given by Ramos et al. [4] with indication of the composition of the RS alloys and type of microstructure after rapid solidification.

Table 1
Phases present in the arc melted spheres and type of microstructure of the RS disks of the Ti–Si–B alloys.

Composition (at%.)	Arc melted sphere	RS disk
$Ti_{85}Si_{15}$	αTi + Ti_5Si_3	Amorphous matrix with nanocrystals
$Ti_{80}Si_{20}$	αTi + Ti_5Si_3	Amorphous matrix with nanocrystals
$Ti_{84}Si_{14}B_2$	αTi + Ti_5Si_3 + Ti_6Si_2B	Amorphous matrix with nanocrystals
$Ti_{82.5}Si_{10}B_{7.5}$	αTi + TiB + Ti_6Si_2B	Amorphous matrix with nanocrystals
$Ti_{80.5}Si_{14.5}B_5$	αTi + Ti_6Si_2B	Amorphous
$Ti_{80}Si_{10}B_{10}$	αTi + TiB + Ti_6Si_2B	Amorphous matrix with nanocrystals
$Ti_{77}Si_{10}B_{13}$	αTi + TiB + TiB_2 + Ti_6Si_2B	Amorphous matrix with nanocrystals
$Ti_{76}Si_{20}B_4$	αTi + Ti_5Si_3 + Ti_6Si_2B	Amorphous matrix with nanocrystals
$Ti_{75}Si_{18}B_7$	αTi + Ti_3Si + Ti_5Si_3 + Ti_6Si_2B	Amorphous
$Ti_{73}Si_{20}B_7$	αTi + Ti_5Si_3 + Ti_6Si_2B	Amorphous matrix with nanocrystals

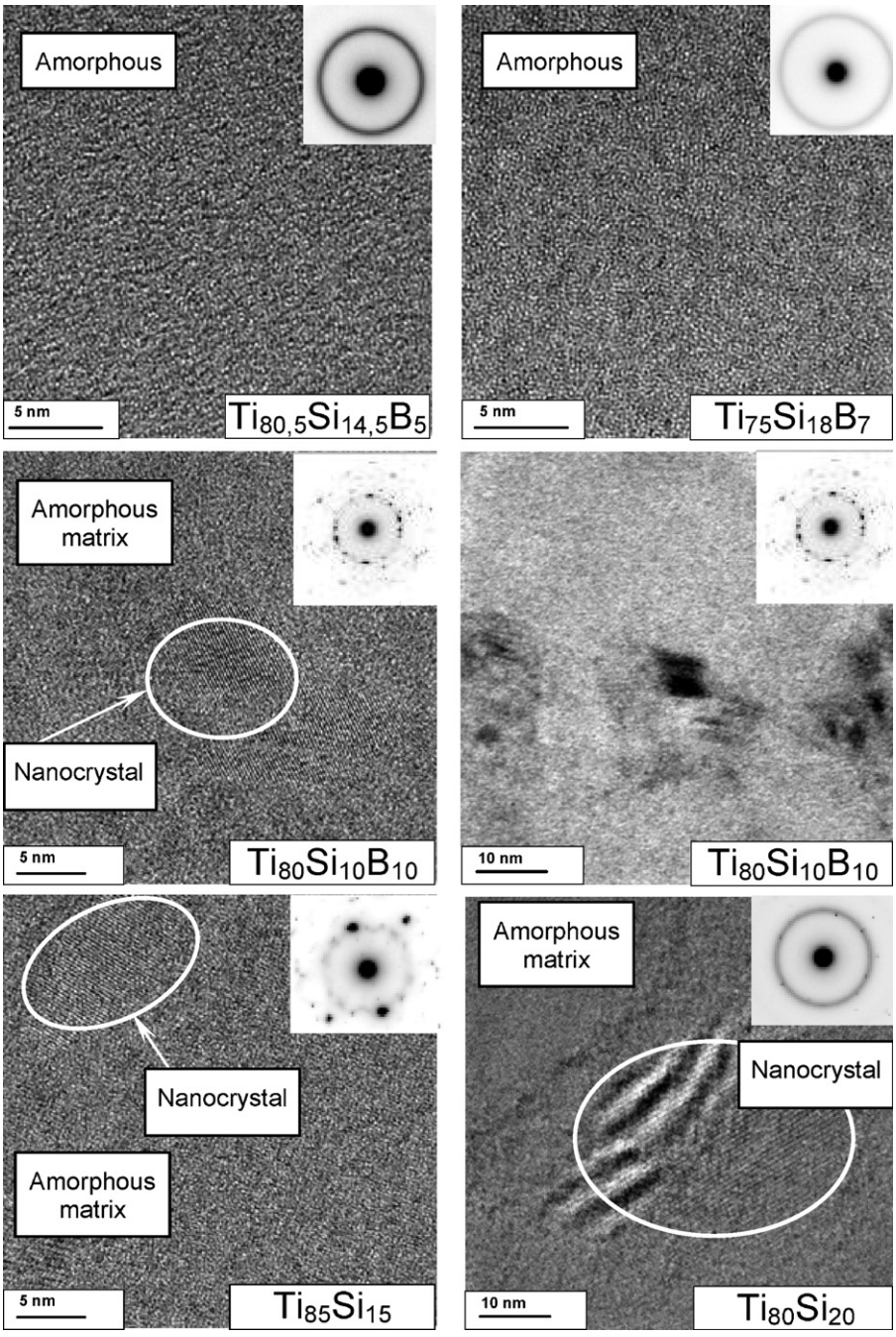

Fig. 3. High resolution transmisson electron microscopy (HRTEM) micrographs of the RS disks.

microstructures were all homogeneous and the largest size of the phases present was around 20 μm.

3.2. Rapidly solidified alloys

The RS disks showed approximately 20 mm in diameter and 50 μm thickness. Fig. 2 and Table 1 shows the compositions of the RS alloys which resulted in either amorphous or amorphous with nanocrystals microstructures after rapid solidification. Rapid solidified samples with compositions outside the region indicated in Fig. 2 were totally crystalline.

Fig. 3 shows several HRTEM (high-resolution and bright field) micrographs of the RS disks and their selected area diffraction pattern. In the cases where nanocrystals were present, it was not possible to identify the correspondent phases via the SAD data.

Note in Fig. 3 that the binaries $Ti_{85}Si_{15}$ and $Ti_{80}Si_{20}$ RS disks presented amorphous matrix with embedded nanocrystals. Suryanarayana et al. [9] indicates the formation of amorphous microstructure for both compositions while Polk et al. [10] inform the formation of amorphous microstructure for $Ti_{80}Si_{20}$ and crystalline for $Ti_{85}Si_{15}$ composition. It should be informed that both authors used the melt spinning technique to produce their alloys.

3.3. Crystallization temperature (Tx)

The crystallization temperature (Tx) of the amorphous phase present in the RS disks were determined from the exothermic peak

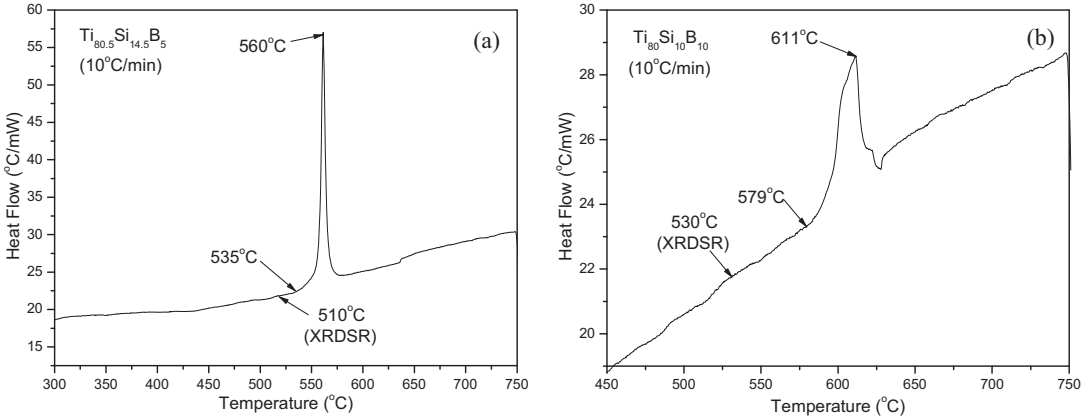

Fig. 4. DSC thermograms from the (a) $Ti_{80}Si_{10}B_{10}$ and (b) $Ti_{84}Si_{14}B_2$ RS disks.

Table 2
Crystallization temperatures (Tx) obtained by DSC and XRDSR and the phases present after crystallization for each alloy composition.

Composition (at.%)	DSC (°C)	XRDSR (°C)	After crystallization (DSC)	After crystallization (XRDSR)
$Ti_{85}Si_{15}$	510–557	–	αTi + Ti_5Si_3 + Ti_3Si	–
$Ti_{80}Si_{20}$	509–551	510	αTi + Ti_5Si_3 + Ti_3Si	–
$Ti_{84}Si_{14}B_2$	546–560	510	αTi + Ti_6Si_2B	αTi + Ti_6Si_2B
$Ti_{82.5}Si_{10}B_{7.5}$	582–612	–	αTi + Ti_6Si_2B	–
$Ti_{80.5}Si_{14.5}B_5$	535–560	510	αTi + Ti_6Si_2B	αTi + Ti_6Si_2B
$Ti_{80}Si_{10}B_{10}$	579–611	530	αTi + Ti_6Si_2B	αTi + Ti_6Si_2B
$Ti_{77}Si_{10}B_{13}$	641–647	550	αTi + TiB + Ti_6Si_2B	αTi + Ti_6Si_2B
$Ti_{76}Si_{20}B_4$	536–566	530	αTi + Ti_5Si_3 + Ti_6Si_2B	αTi + Ti_6Si_2B
$Ti_{75}Si_{18}B_7$	533–565	530	–	αTi + Ti_6Si_2B
$Ti_{73}Si_{20}B_7$	550–608	–	αTi + Ti_5Si_3 + Ti_6Si_2B	–

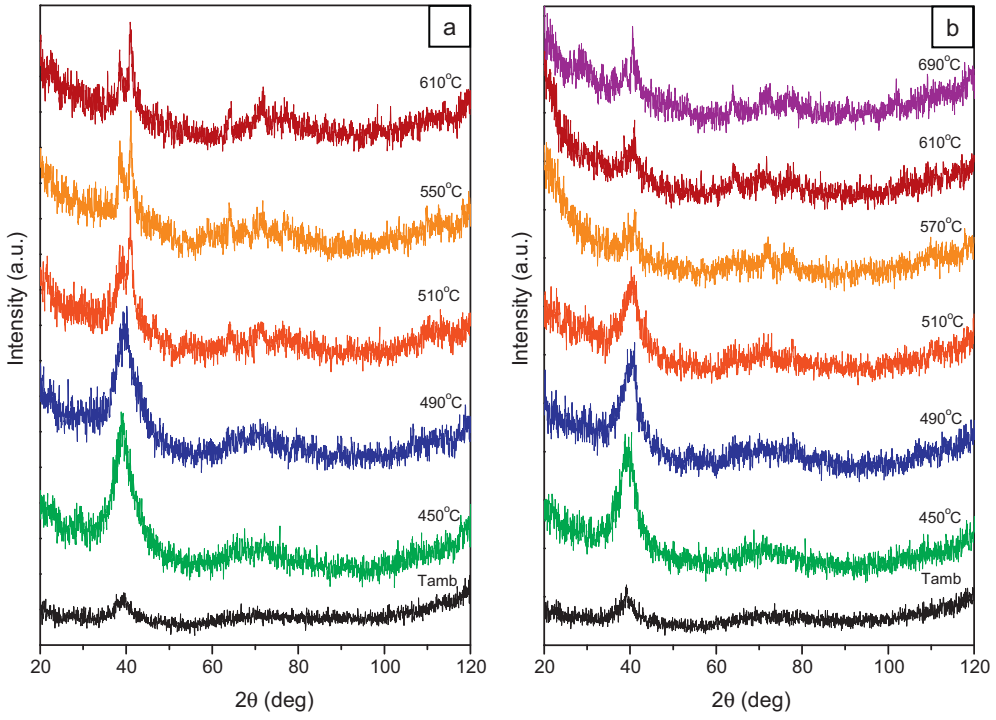

Fig. 5. XRDSR diffractograms from the RS disks (a) $Ti_{80.5}Si_{14.5}B_5$ alloy composition and (b) $Ti_{80}Si_{10}B_{10}$ alloy composition.

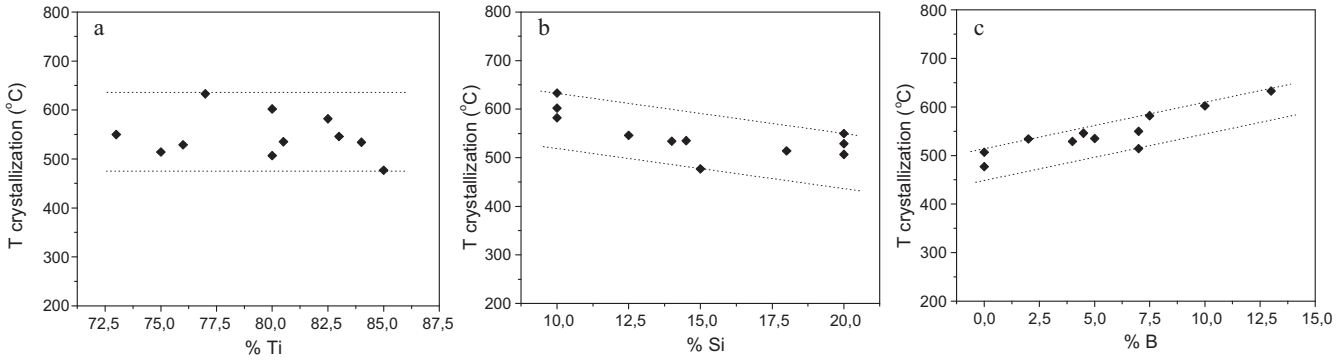

Fig. 6. Crystallization temperature (Tx) as a function of (a) Ti, (b) Si and (c) B content of the RS disks.

presented in the DSC thermograms and High Temperature X-ray diffraction synchrotron radiation (XRDSR) experiments. In the DSC experiments, all compositions showed only one peak up to the maximum heating temperature (750 °C), indicating crystallization in a single stage. Table 2 shows the crystallization temperatures (Tx) obtained by DSC and XRDSR and the phases present after crystallization for each alloy composition, based on the significant X-ray diffraction intensity reflections.

The initial crystallization temperatures (Tx) of the RS binary disks $Ti_{85}Si_{15}$ and $Ti_{80}Si_{20}$ were 510 and 509 °C respectively, αTi, Ti_5Si_3 and Ti_3Si phases were observed after crystallization of both compositions. According to Suryanarayana et al. [9], the crystallization should occur in two stages, with crystallization temperatures of 429 and 537 °C for the $Ti_{85}Si_{15}$ alloy and 429 and 544 °C for the $Ti_{80}Si_{20}$ alloy. The first stage involved the precipitation of bcc β-Ti solid solution and the second stage showed the precipitation of the metastable Ti_5Si_3 phase. Polk et al. [10] inform a crystallization temperature of 594 °C for the $Ti_{80}Si_{20}$ composition, but it is not informed the phases formed after crystallization.

Table 3
Phases presents in the RS disks after heat treatment at 700 °C for 120 h.

Composition (at.%)	RS disk	After heat treatment
$Ti_{80}Si_{20}$	Amorphous matrix with nanocrystals	αTi + Ti_3Si
$Ti_{84}Si_{14}B_2$	Amorphous matrix with nanocrystals	αTi + Ti_3Si + Ti_6Si_2B
$Ti_{82.5}Si_{10}B_{7.5}$	Amorphous matrix with nanocrystals	αTi + Ti_6Si_2B
$Ti_{80.5}Si_{14.5}B_5$	Amorphous	αTi + Ti_6Si_2B
$Ti_{80}Si_{10}B_{10}$	Amorphous matrix with nanocrystals	αTi + Ti_6Si_2B
$Ti_{77}Si_{10}B_{13}$	Amorphous matrix with nanocrystals	αTi + TiB + Ti_6Si_2B
$Ti_{76}Si_{20}B_4$	Amorphous matrix with nanocrystals	αTi + Ti_3Si + Ti_6Si_2B

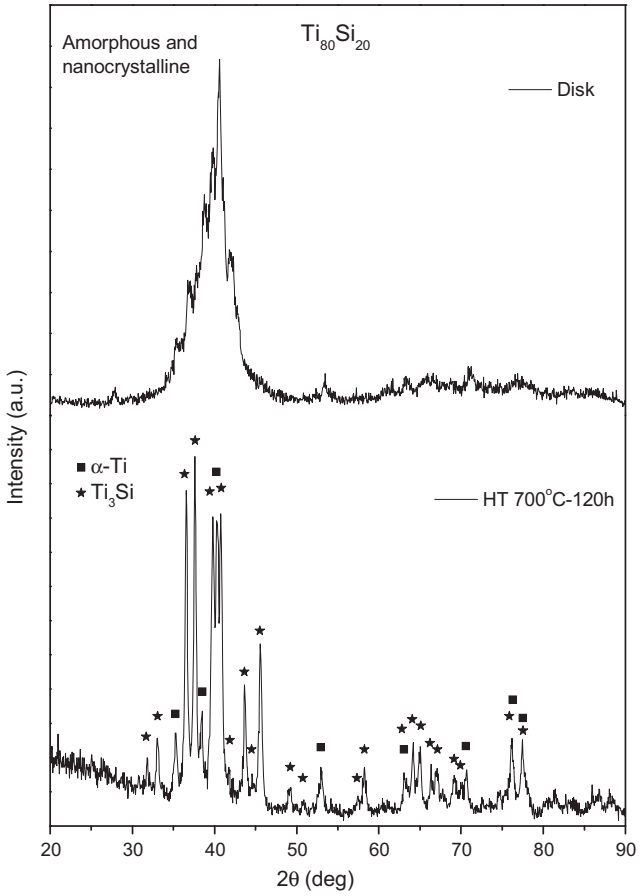

Fig. 7. X-ray diffraction pattern of $Ti_{80}Si_{20}$ alloy.

Fig. 4 shows DSC thermograms of the $Ti_{80.5}Si1_{4.5}B_5$ and $Ti_{80}Si_{10}B_{10}$ RS disks. In the thermograms it is also indicated the first temperature where crystalline peaks were observed from the XRDSR measurements, noting that the temperatures obtained via XRDSR were found close to those from DSC (Table 2). Fig. 5 shows XRDSR diffractograms of the $Ti_{80.5}Si_{14.5}B_5$ and $Ti_{80}Si_{10}B_{10}$ RS disks after heating up to 750 °C. Fig. 6 shows graphs of crystallization temperature (Tx) as a function of Ti, Si and B contents of the RS

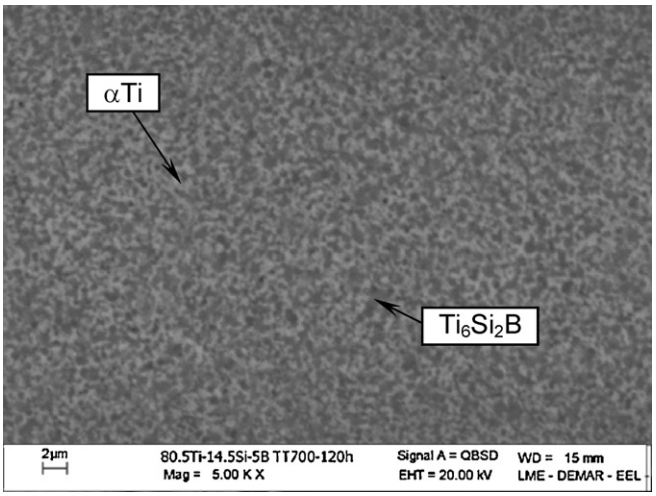

Fig. 8. Micrograph of the $Ti_{80.5}Si_{14.5}B_5$ alloy via SEM/BSE after heat treatment at 700 °C for 120 h.

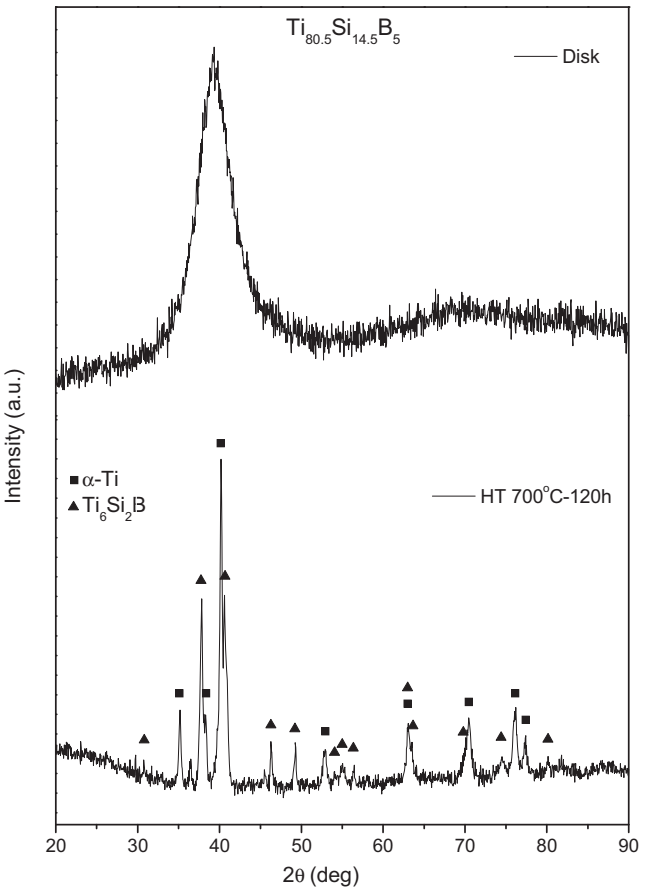

Fig. 9. X-ray diffraction pattern of $Ti_{80.5}Si_{14.5}B_5$ alloy.

disks. It was noted a trend in decrease of Tx for higher Si contents and an increase of Tx for higher B contents.

After DSC and XRDSR, all the alloys presented crystalline and basically formed by two or three of the following phases: αTi, Ti_6Si_2B; Ti_5Si_3; Ti_3Si and TiB.

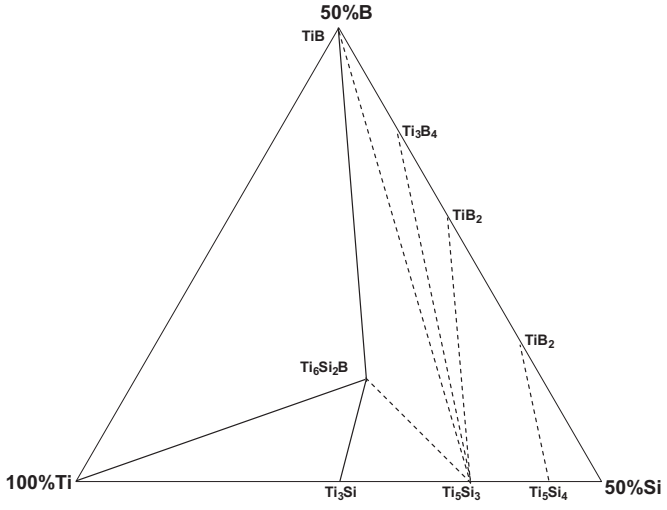

Fig. 10. Proposed isotherm section at 700 °C for the Ti–Si–B system.

3.4. Thermal stability at 700 °C

Table 3 shows the phases present in the disks after heat treatment at 700 °C for 120 h, based on the significant X-ray diffraction intensity reflections and micrographs obtained by SEM/BSE. Fig. 7 shows the X-ray diffraction patterns of $Ti_{80}Si_{20}$ sample which confirms the stability of the αTi + Ti_3Si two-phase field at 700 °C in line with the recent results of Costa et al. [11]. It has been shown the stability of the Ti_6Si_2B at 700 °C, a phase which is likely stable up to room temperature. Fig. 8 shows a SEM/BSE micrograph and Fig. 9 the X-ray diffraction pattern of $Ti_{80.5}Si_{14.5}B_5$ RS disk after HT at 700 °C for 120 h. Considering these results, Fig. 10 shows a proposed isotherm section at 700 °C for the Ti–Si–B system.

4. Summary

This investigation focused on rapid solidification of Ti-rich Ti–Si–B alloys via splat-cooling and evaluation of phase stability at 700 °C from the rapidly solidified alloys. As expected, rapid solidification promoted significant refinement of the microstructures. Amorphous and amorphous with embedded nanocrystals have been observed after rapid solidification from specific alloy compositions. The values of the crystallization temperature (Tx) of the alloys were in the 509–647 °C temperature range. After Differential Scanning Calorimetry and High Temperature X-ray Diffraction with Synchrotron radiation, the alloys showed crystalline and basically formed by two or three of the following phases: αTi, Ti_6Si_2B; Ti_5Si_3; Ti_3Si and TiB. It has been shown the stability of the Ti_3Si and Ti_6Si_2B phases at 700 °C and the proposition of an isothermal section at this temperature.

Acknowledgements

The authors acknowledge the financial support of CNPq (# 142242/2007-1), FAPESP (#. 2001/09529-7, # 2007/05206-5), FINEP (# 1651) and Brazilian Synchrotron Light Laboratory (LNLS) for the HRTEM and XRDSR experiments.

References

[1] S.H. Whang, Journal of Materials Science 21 (1986) 2224–2238.
[2] J.D. Destefani, ASM International Handbook, Vol. 2, Properties and selection: Nonferrous alloys and special-purpose materials, vol. 594, 1990, pp. 586–591.
[3] C.G. McKamey, S.H. Whang, C.T. Liu, Scripta Metallurgica et Materialia 32 (1995) 383–388.
[4] A. S. Ramos, "Determinação da seção isotérmica a 1250 °C e da projeção liquidus do sistema Ti–B–Si na região delimitada por 100%Ti–80%Si–80%B", 2001, Ph.D. Thesis (Doutorado em Engenharia de Materiais) – Departamento de Engenharia de Materiais, EEL-USP, Lorena-SP.
[5] A.S. Ramos, C.A. Nunes, G. Rodriguez, P.A. Suzuki, G.C. Coelho, A. Grytsiv, P. Rogl, Intermetallics 12 (2004) 487–491.
[6] Y Yang, Y.A. Chang, L. Tan, Intermetallics 13 (2005) 1110–1115.
[7] T. Zhang, A. Inoue, T. Masumoto, Materials Science and Engineering A 181/182 (1994) 1423–1426.
[8] S.M.L. Sastry, T.C. Peng, P.J. Meschter, J.E. O'Neil, Journal of Metals 35 (1983) 21–24.
[9] C. Suryanarayana, A. Inoue, T. Masumoto, Journal of Materials Science 15 (1980) 1993–2000.
[10] D.E. Polk, A. Calka, B.C. Giessen, Acta Metallurgica 26 (1978) 1097–1103.
[11] A.M.S. Costa, G.F. Lima, G. Rodrigues, C.A. Nunes, G.C. Coelho, P.A. Suzuki, Journal of Phase Equilibria and Diffusion 31 (2010) 22–27.
[12] N. Massaki, T. Okada, Materials Science and Engineering A 178/180 (1994) 366–370.
[13] G.F. Lima, A.M.S. Costa, P.A. Suzuki, C.A. Nunes, G.C. Coelho, Materials Characterization 59 (2008) 1753–1756.